

MICROSTRUCTURE AND PROPERTIES OF COMPOSITE COATINGS OBTAINED ON ALUMINIUM ALLOYS

This paper presents methods of modifying the anode surface layers of Al_2O_3 by introducing carbon to their microstructure. Composite coatings were prepared using two different methods. In the first, coatings were formed by means of oxidation under constant current conditions. Anodic oxidation of aluminium was conducted in a multicomponent electrolyte with the addition of organic acids and graphite. The second method was based on the formation of oxide coatings in an electrolyte without the addition of graphite or heat treatment of the layers of succinic acid. The obtained coatings were tested using SEM, TEM, and GDOES (glow discharge optical emission spectrometry) and their tribological and stereometric properties were measured. The study demonstrated the beneficial effects of the methods when used to improve the tribological properties of sliding couples.

Keywords: composite coatings, hard anodising, Al_2O_3

1. Introduction

The oxide coatings formed on aluminium alloys exhibit good tribological properties when working with polymers in oil-free systems. However, the resistance to movement resulting from the cooperation of components in a kinematic system affects the wear of the polymer sliding partner [1]. Attempts are being made to reduce the wear of the polymer in these systems by introducing additives which facilitate the formation of a sliding polymer film on the surface of a hard oxide coating. This is achieved through modification of the tribological partners – most often polymers, which are modified by solid lubricant additives (carbon, MoS_2) [2] or so-called friction polymers (PTFE) [3] as dispersive components in the form of flakes, particles, or fibres [4]. There are numerous potential methods of modifying anodic hard coatings. Improvement of the tribological properties of these coatings can be achieved by changing the fabrication parameters (current and temperature conditions of the process, electrolyte composition) [5] or by introducing a composite component into the microstructure of the oxide [6]. Changing the fabrication parameters directly influences the thickness and microhardness of the coatings along with their microstructure and surface morphology [7–9]. Due to its porous microstructure, the anodic hard coating produced on aluminium using electrochemical methods facilitates its use as a matrix for composite coatings. Composite coatings based on anodic hard coatings can be obtained using a number of methods, including electrochemical, CVD, PVD, and their variants [10–12]. Metals (Ni, Cu, Cr, Co) are used most often as modifiers of aluminium oxide coatings for tribological purposes [13,14], followed by low-friction polymers (PU, PTFE) [15,16] and solid lubricants (C, MoS_2 , WS₂) [17–19]. The modifiers fill in the porous microstructure of the Al_2O_3 coating and take over part of the dynamic load, thereby

protecting the oxide coating against cracking. It is most advantageous for anodic hard coatings intended for sliding interaction with polymers to be modified with solid lubricants. This enables a reduction in the value of tangent forces acting on a couple and thus the achievement of lower values of friction forces and less wear of the friction couple (mostly the polymer). In this paper, the authors present two modifications of an anodic hard coating intended for sliding oil-free interaction with low-friction polymers. The modifications consist of introducing carbon coatings into the microstructure and onto the surface. The purpose is to achieve a reduction in the friction force and wear of the polymer interacting with the coatings. The proposed modifications can be applied in oil-free piston-cylinder systems (air compressors, pneumatic servomotors).

2. Research material

All samples for the research were made from a rolled sheet of the aluminium alloy EN AW-5251. Composite coatings for microscopic examination were deposited on plates with an area of $5 \cdot 10^{-4} \text{ m}^2$; for the examination of chemical element contents, on plates with an area of $4 \cdot 10^{-4} \text{ m}^2$; and for the examination of tribological and stereometric properties, on plates with an area of $1 \cdot 10^{-3} \text{ m}^2$. Prior to anodising, the surfaces of all the samples were etched in a 5 % KOH solution, rinsed in distilled water, and subjected to neutralisation in a 10 % HNO_3 solution. The composite coatings were prepared using two different methods (Table 1). In the first, the coatings were formed by means of oxidation under constant current conditions. The anodic oxidation of aluminium was conducted in a multicomponent electrolyte with the addition of organic acids and graphite, with a content of 30 g/dm^3 of the electrolyte at constant

* UNIVERSITY OF SILESIA IN KATOWICE, INSTITUTE OF TECHNOLOGY AND MECHATRONICS, SOSNOWIEC, POLAND

Corresponding author: tomasz.kmita@us.eu.pl

current density parameters of 2 or 3 A/dm², in a bath at 303 K. For the modification, graphite powder with a purity level of 99 % and an average grain size below 1 μm was used. The second method was based on the formation of oxide coatings in an electrolyte without the addition of graphite or heat treatment of succinic acid layers. The oxidation was conducted at a current density of 3 A/dm² at temperatures of 293 and 303 K. The process of sealing was carried out for 30 minutes at 373 K and for 20 minutes at 368 K.

The coatings formed by anodising were rinsed in distilled water for 1 h in order to remove the remaining electrolyte from their porous structure.

The tribological partner in the sliding couple with the composite coatings was a pin, 9·10⁻³ m in diameter, made of PEEK/BG. The PEEK/BG composite contains dispersive phases in the form of PTFE fibres, graphite flakes and carbon fibres (Fig. 1), ensuring high dimensional stability (25·10⁶ m/m·K), low absorbability (0.14 %), and reduced resistance to movement in sliding couples.

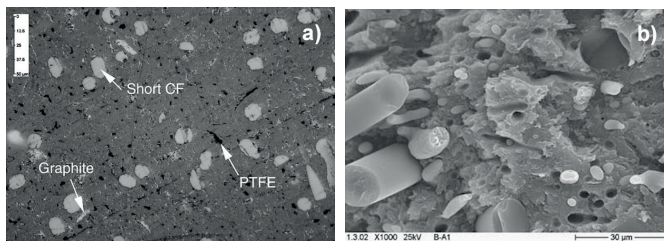


Fig. 1. PEEK/BG: a) cross section, b) fracture [4]

The PEEK/BG composite material is also characterised by high levels of mechanical strength, stiffness, and hardness, as well as good creep and abrasion resistance. Owing to these properties, PEEK/BG is widely applied in oil-free sliding couples.

3. Research methodology

The surface morphology of the composite coatings was examined with a Philips XL30 scanning electron microscope. Since amorphous aluminium oxide does not allow electrons knocked off by a microscopy beam to be drawn off, the tested coatings were first sputtered with gold. The sputtering operation was performed with a Gatan 682 PECS device. For current conditions of $V = 10$ keV, $I = 400$ μA, the sputtering rate was $t = 3$ Å/s. Sputtering was conducted until the thickness of the Ag-Pd layer reached 0.5 kÅ.

Examination of the structure of the composite coatings was carried out with a JEM-2010 ARP transmission microscope, using a Gatan Orius CCD high-resolution video camera with resolving power of 0.194 nm, fitted with a scanning transmission (STEM) attachment with accelerating voltage of 200 kV. Tests were performed on cross sections of the samples.

Changes in elemental composition deep within the composite coating were determined with a JY 10000 RF spectrometer using radio frequency (RF) glow discharge optical emission spectrometry (GDOES). Quantitative analyses were made of the concentration of given elements, expressed in atomic percentage as a function of depth expressed in micrometres.

Friction and wear tests were carried out using a T-17 tester in a pin-on-plate sliding couple in a reciprocating motion. The tests were performed under conditions of technically dry friction, at an ambient temperature of 296 ± 1 K and relative air humidity of 30 ± 5 %. Constant values of unit pressure (0.5 MPa) and of average sliding speed (0.2 m/s) were applied for all of the investigated couples. The tests were carried out over a distance of 1.5 km in four stages, after which the mass of the pin was measured. Friction force was measured by means of a Spider 8 analogue-to-digital converter, using a sampling rate of 50 Hz.

Examination of the geometrical structure of the surface before and after the tribological test was performed with a Form Talysurf Series 2 contact profilographometer, using the 3D method. The thickness of the layers was measured with a Dualscope thickness gauge, using the eddy current method.

4. Research results

As a result of the conducted anodising of the aluminium alloy surface, oxide coatings with a thickness of 50 ± 2 μm were obtained. Examination of the microstructure of the unmodified coatings (sample A) showed the fibrous structure of the Al₂O₃ coatings. The aluminium oxide fibres are oriented perpendicularly to the substrate surface, along the direction of coating growth. The spaces between the oxide fibres form channels for oxygen ions which combine with aluminium ions in the electrochemical process (Fig. 2a). Surface nanoporosity, characteristic of aluminium oxides, is an effect of the columnar structure of the coatings (Fig. 2b). The nanopores are formed as a result of aluminium oxide fibres contacting one another and are present in all cross sections of the fibres throughout the coating thickness. There is no visible dispersion in the microstructure of the unmodified coatings.

TABLE 1

Parameters of formation of composite coatings

Feature	Anodising parameters				Thermochemical treatment parameters		
	Modifier	Current density [A/dm ²]	Temperature [K]	Time [h]	Modifier	Temperature [K]	Time [h]
A	–	3	303	1	–	–	–
G2	C (graphite)	2	303	1	–	–	–
G3		3	303	1	–	–	–
U20	–	3	293	1	(CH ₂ COOH) ₂	373	30
U30	–	3	303	1	–	368	20

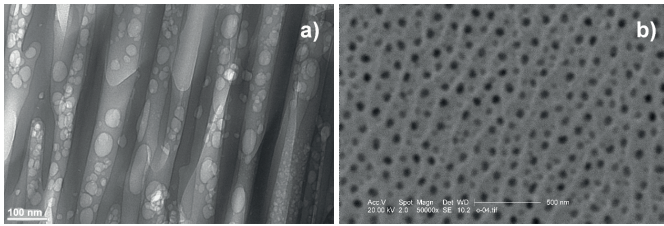


Fig. 2. Images of: a) the microstructure of the unmodified oxide coating and b) the surface morphology (sample A)

Analysis of microscopic images of the composite coatings formed in an electrolyte with the addition of organic acids and graphite (samples G2 and G3) showed the presence of carbon precipitates in the microstructure of the coatings (Fig. 3).

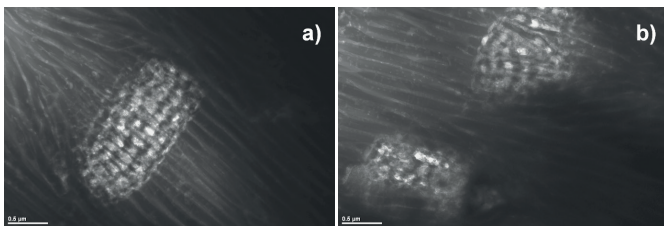


Fig. 3. Images of the microstructure of an oxide coating modified with graphite: a) sample G2, b) sample G3

The precipitates are deposited between oxide fibres so that the latter surround the graphite grains. The gradation of the graphite grains identified in the coating microstructure amounts to $<1 \mu\text{m}$. The size of the precipitates is identical to that of the graphite powder used to produce the electrolyte. The analysis of images of the surface morphology of the composite coatings showed no carbon precipitates on the surface of the samples.

At the same time, the analysis of surface images of the composite coatings formed in an electrolyte not modified with graphite before thermochemical treatment (Fig. 4a, b) showed the influence of the temperature of the process on the stereological parameters. The Al_2O_3 coatings produced at a temperature of 293 K were characterised by a lower area fraction of porosity (9.8 %) compared to those produced at 303 K (15.1 %). This is because the solubility of aluminium oxide in the electrolyte increases as the temperature of the electrolyte grows. The analysis of surface images of the coatings formed in an electrolyte not modified with graphite after thermochemical treatment in succinic acid (Fig. 5a, b) showed the presence of precipitates partly covering the surface of the coatings.

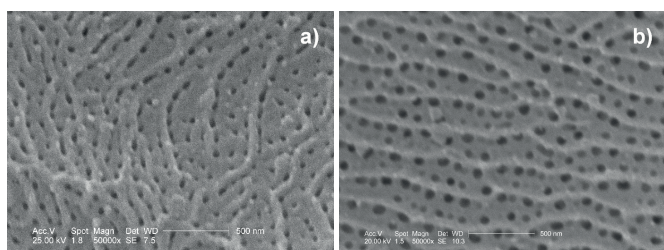


Fig. 4. Image of the surface morphology of the oxide coating before thermochemical treatment in succinic acid: a) sample U20, b) sample U30

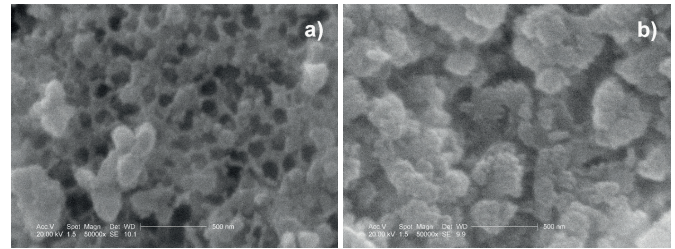


Fig. 5. Image of the surface morphology of the oxide coating after thermochemical treatment in succinic acid: a) sample U20, b) sample U30

The effect of the modification of Al_2O_3 coatings by means of thermochemical treatment in succinic acid also applies to their microstructure. As a result of the applied modification, swelling of the aluminium oxide fibres can be observed (Fig. 6a, b).

GDOES analyses of the elemental composition of the coatings show changes in the contents of the elements analysed as a function of the depth of the layer from the surface. In the near-surface region, increased carbon content is observed in all of the analysed Al_2O_3 coatings. This can be attributed to gaseous impurities. The carbon content in the subsurface region decreases rapidly as the distance from the surface increases.

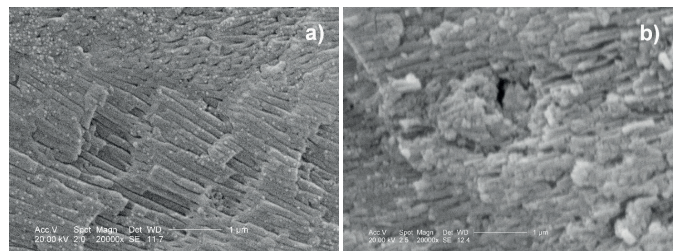


Fig. 6. Image of the microstructure of an oxide coating a) before and b) after thermochemical treatment in succinic acid (sample U20)

Decreasing oxygen content and increasing aluminium content are also observable. The microstructure in the central part of the coating shows the stoichiometric relationship of the elemental composition of aluminium oxide. Near the substrate of the coating, a reverse dependence is observed compared to the surface. The oxygen content decreases, whereas the aluminium content increases. The unmodified coating (Fig. 7a) contains only 14 % carbon in the near-surface region, whereas all of the modified coatings show much higher carbon content in this region. Analysis of the coatings modified with graphite (Fig. 7b, c) showed 52 % (sample G2) and 45 % of carbon (sample G3). Carbon was identified in the microstructure of the coatings to depths of $4.7 \mu\text{m}$ (sample G2) and $3.8 \mu\text{m}$ (sample G3). In the case of the coatings modified by means of thermochemical treatment in succinic acid (Fig. 8a, b), carbon content in the microstructure was 62 % (sample U20) and 55 % (sample U30). For this modification, the depth to which carbon was identified was $4.8 \mu\text{m}$ (sample U20) and $4.2 \mu\text{m}$ (sample U30).

As a result of the friction/wear tests of a couple consisting of the coatings with PEEK/BG, the application of a polymer

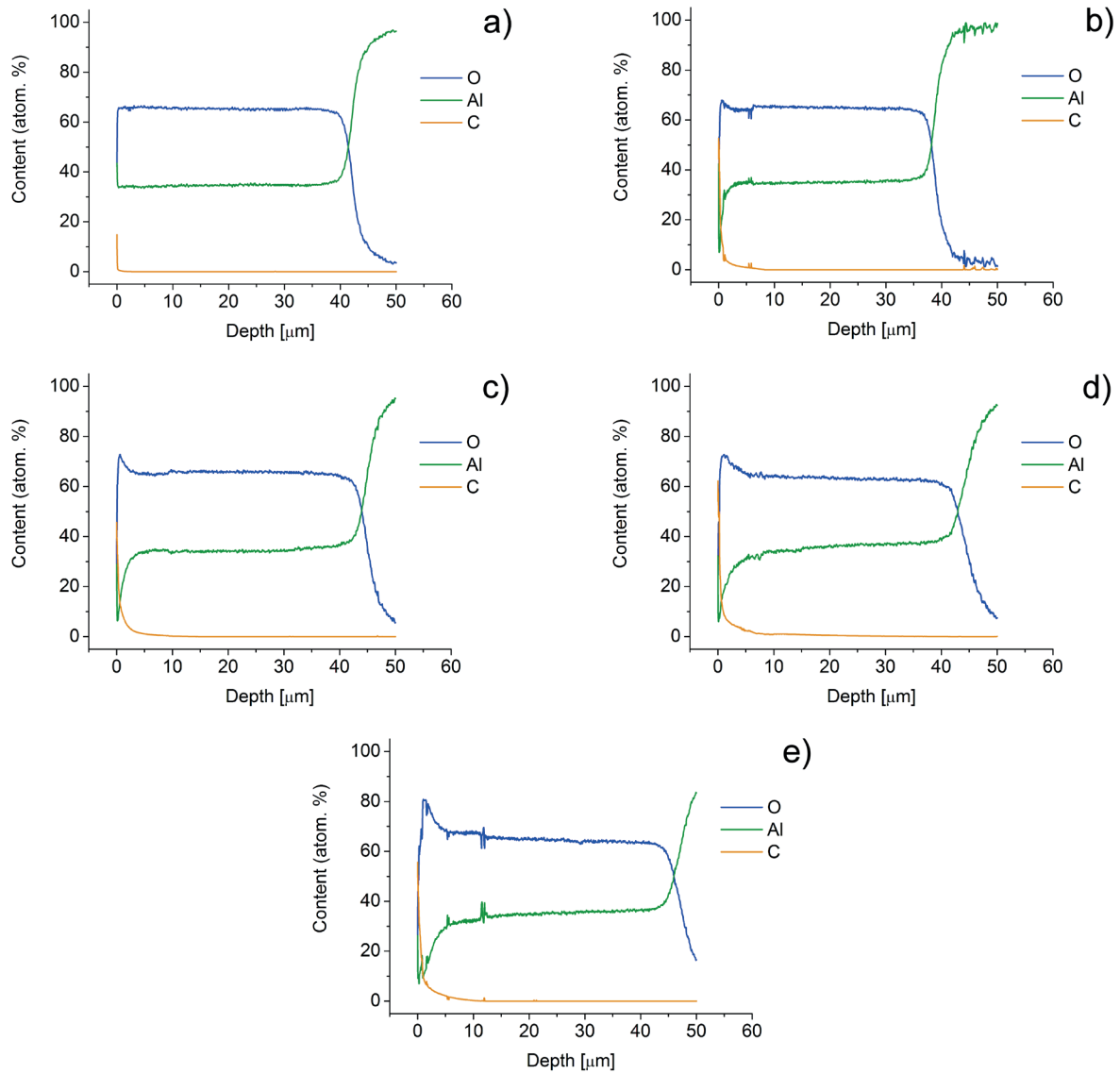


Fig. 7. GDOES analysis of the coating: a) without modification (A), b) modified with graphite (G2), c) modified with graphite (G3), d) modified by means of thermochemical treatment in succinic acid (U20), e) modified by means of thermochemical treatment in succinic acid (U30)

sliding film to the Al₂O₃ surface was observed. Tribological tests showed a slight decrease (to 15 %) in the friction coefficient (Fig. 8a) and a considerable decrease (to 74 %) in the PEEK/BG wear intensity when working in a couple with the modified coatings (Fig. 8b), compared to the couples with the reference coating.

Examination of the geometrical structure of the surface of the coatings performed prior to the tribological test show lower values of amplitude parameters, Sq, of the modified coatings compared to the reference coating (Fig. 9a). In particular, the coatings modified by means of thermochemical treatment show lower values of this parameter. This results

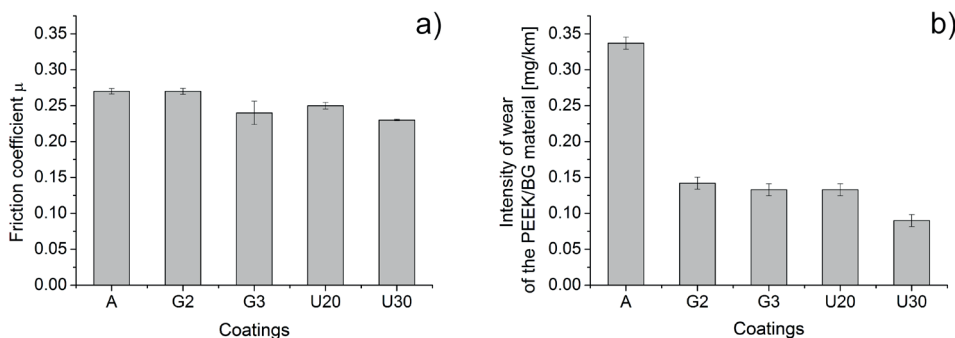


Fig. 8. Tribological test parameters: a) friction coefficient, b) wear intensity of the PEEK/BG polymer

from the presence of precipitates of the thermochemical treatment which wholly or partly seal the surface irregularities of the oxide coating. However, this method of modification leads to the formation of a surface which is less predisposed to work in sliding couples, as corroborated by the value of parameter Ssk (Fig. 9b). Examination of surface topography carried out after the tribological test revealed differences in the nature of the deposition of a sliding film on the coatings modified by means of thermochemical treatment compared to the unmodified coatings as well as to those modified with graphite. This is manifested, in particular, in the lower values of the Sq parameter for the coatings modified by means of thermochemical treatment. Following the tribological test, the unmodified coatings and those modified with graphite show a change in geometrical structure typical of coatings

after the wearing-in process. This is visible in the lower values of parameters Sq and Ssk. In the case of coatings modified by means of thermochemical treatment, the lower values of Sq are not accompanied by decreased values of the Ssk parameter. This can be explained by the lower value of hardness of the precipitates formed on the surface of the coatings resulting from thermochemical treatment, compared to the surface hardness of other coatings. The axonometric images of the surfaces corroborate this thesis (Fig. 10d, e). The images show scratches in directions consistent with the reciprocating motion of the cooperating surfaces. This directionality is not observable on the images of the coatings modified with graphite or of the unmodified coatings (Fig. 10a–c). In the case of the coatings modified with graphite, there are no significant differences in the geometrical

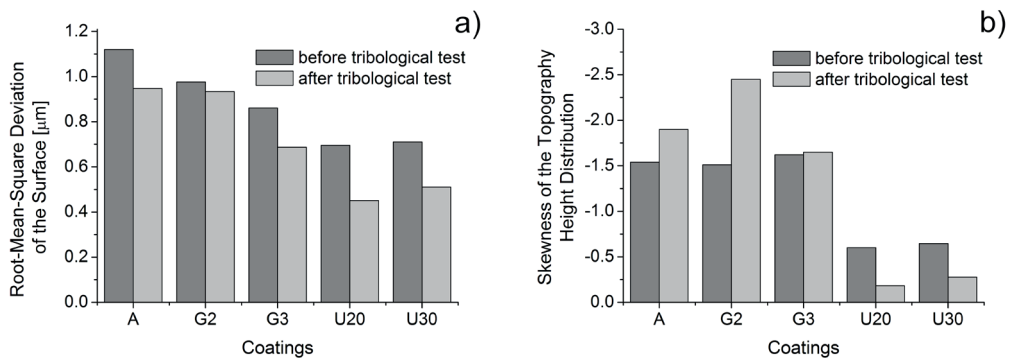


Fig. 9. Geometrical structure of the coating surface: a) root-mean-square deviation of the surface, Sq, b) skewness of topography height distribution, Ssk

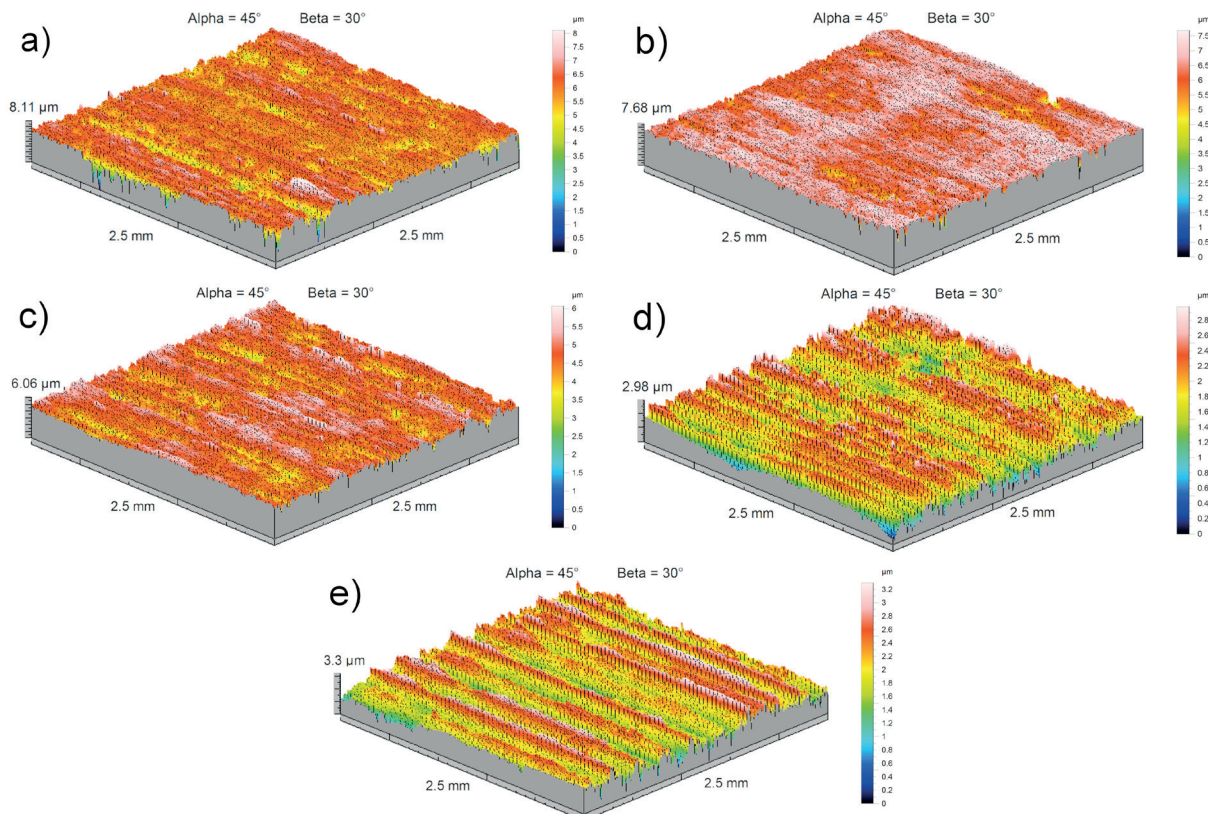


Fig. 10. Axonometric images of coating surfaces after the tribological test: a) sample A, b) sample G2, c) sample G3, d) sample U20, e) sample U30

structure of the surface compared to the reference sample, due to the fact that a majority of the graphite grains were built into the coating microstructure.

5. Conclusions

Based on the research and analysis of the results, it can be concluded that:

1. The composite coatings formed in an electrolyte with a graphite additive and subjected to thermochemical treatment in succinic acid are characterised by increased contents of carbon compounds.
2. In the case of the coatings produced in an electrolyte with a graphite additive, the graphite grains are built into the oxygen microstructure. In the coatings subjected to sealing, carbon precipitates are surface-structural in nature.
3. The composite coatings show a slight reduction in the friction coefficient in a couple with PEEK/BG and a significant decrease in the intensity of PEEK/BG wear during tribological interaction.
4. The proposed modifications to the Al₂O₃ coating exert a favourable influence on the geometrical structure of the coating surface.

REFERENCES

- [1] W. Skoneczny, *MATER SCI+*. 50, (3), 435–442 (2014).
- [2] Y. Tang, J. Yang, L. Yin, B. Chen, H. Tang, C. Liu, Ch. Li, *COLLOID SURFACE A*. 459, 261–266 (2014).
- [3] D. L. Burris, W. G. Sawyer, *WEAR*. 261, (3–4), 410–418 (2006).
- [4] Z. Zhang, C. Breidt, L. Chang, K. Friedrich, *TRIBOL INT*. 37, (3), 271–277 (2004).
- [5] T. Kmita, W. Skoneczny, *EKSPLOAT NIEZAWOD*. 45, (1), 77–82 (2010).
- [6] A. Posmyk, H. Wistuba, *ARCH METALL MATER*. 56, (4), 909–917 (2011).
- [7] Y. Jia, H. Zhou, P. Luo, S. Luo, J. Chen, Y. Kuang, *SURF COAT TECH*. 201, (3–4), 513–518 (2006).
- [8] L. E. Fratila-Apachitei, F. D. Tichelaar, G. E. Thompson, H. Terryn, P. Skeldon, J. Duszczyk, L. Katgerman, *ELECTROCHIM ACTA*. 49, (19), 3169–3177 (2004).
- [9] M. F. Morks, A. S. Hamdy, N. F. Fahim, M. A. Shoeib, *SURF COAT TECH*. 200, (16–17), 5071–5076 (2006).
- [10] A. Hajian, A. A. Rafati, A. Afraz, M. Najafi, *J MOL LIQ*. 199, 150–155 (2014).
- [11] G. Służalek, P. Duda, H. Wistuba, *SOL ST PH*. 199, 209–216 (2013).
- [12] M. Pisarek, R. Nowakowski, A. Kudelski, M. Holdynski, A. Roguska, M. Janik-Czachor, E. Kurowska-Tabor, G. D. Sulka, *APPL SURF SCI*. 357, 1736–1742 (2015).
- [13] A. Posmyk, *SURF COAT TECH*. 206, (15), 3342–3349 (2012).
- [14] W. Gumowska, I. Dobosz, M. Uhlemann, J. Koza, *ARCH METALL MATER*. 54, (4), 1119–1133 (2009).
- [15] X. Zhao, W. Li, *SURF COAT TECH*. 200, (11), 3492–3495 (2006).
- [16] H. Wang, H. Yi, H. Wang, *APPL SURF SCI*, 252, (5), 1662–1667 (2005).
- [17] M. Bara, W. Skoneczny, M. Hajduga, *CHEM PROCESS ENG–INZ*. 30, (3), 431–442 (2009).
- [18] J. Sun, L. Weng, Q. Xue, *VACUUM*, 62, (4), 337–343 (2001).
- [19] J. Korzekwa, R. Tenne, W. Skoneczny, G. Dercz, *PHYS STATUS SOLIDI A*. 210, (11), 2292–2297 (2013).